$Cp_2M_2(CO)_4$—Quadruply Bridging, Doubly Bridging, Semibridging, or Nonbridging?

Eluvathingal D. Jemmis, Allan R. Pinhas, and Roald Hoffmann*

Contribution from the Department of Chemistry, Cornell University, Ithaca, New York 14853. *Received September 20, 1979*

Abstract: Electronic structures of alternative geometries of complexes represented by the molecular formula $Cp_2M_2(CO)_4$ are analyzed using the fragment molecular orbital approach. The tendency for CO semibridging found in d^5-d^5 complexes is traced back to $M_2(CO)_{10}$ via a hypothetical nonbridged $Cp_2M_2(CO)_4$ structure. In d^7-d^7 complexes the transformation from the doubly bridging structure to either a nonbridging or a tetrabridging structure is symmetry allowed. The rotational barrier around the M–M bond in the nonbridging structure is calculated to be low, supporting the mechanism of carbonyl scrambling via nonbridging intermediates. An explanation is also offered for the puckering of the $M_2(CO)_2$ rhomboid in *cis*-$Cp_2Fe_2(CO)_4$.

The subject of this paper is the class of binuclear transition metal complexes which contain two metals, two η^5-cyclopentadienyls, and four carbonyls, $Cp_2M_2(CO)_4$. Two distinct structural types are represented among these—cis and trans isomeric compounds with two bridging and two terminal carbonyls, **1**,[1] and **2**, with four semibridging carbonyls.[2] A third

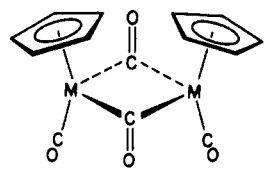

1 cis

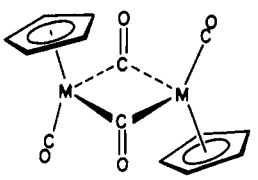

1 trans

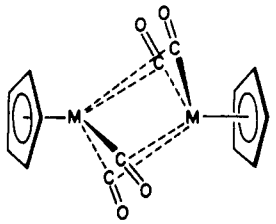

2

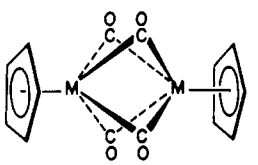

3

structural type, **3**, four carbonyls in the bridge, has not yet been observed.

The nature of the metal–metal bond, the tendency to bridge or not to bridge, what makes for a semibridging interaction, conformational mobility of carbonyls—these are obvious questions that come to mind about these lovely molecules. These queries also reflect some of the more intriguing currents in contemporary organometallic and inorganic chemistry. We will try to make a minor contribution here in unraveling some aspects of the electronic structure of these molecules.

Electron Counting Preliminaries

The thread of a metal–metal bond, of multiplicity to be defined, runs throughout literature discussions (and the structural formula representations) of binuclear complexes in general, and these molecules in particular. So perhaps it is worth repeating explicitly the imperatives of the 18-electron rule, spin state, and bond length which are behind the generally accepted bond multiplicity assignments in these complexes.

$Cp_2Fe_2(CO)_4$, iron formally in oxidation +1 if the Cp ring is taken as anionic, 0 if Cp is a neutral five-electron donor, acquires a 17-electron count around the iron. With a single iron–iron bond in the complex both metals achieve an 18-electron configuration, consistent with the diamagnetic character of the compound. The iron–iron distance in the multitude of complexes whose crystal structure is known ranges between 2.49 and 2.57 Å.[1] Some case could be made for an Fe–Fe single bond on this basis but it is not an awfully strong one.

Replacement of the bridging or terminal carbonyls by linear nitrosyls, cyanide, or isocyanide groups, of terminal carbonyls by phosphines, of a Cp ring by a trio of carbonyls—all of these are relatively trivial electronic perturbations, and the doubly bridged structure **1** is maintained, for iron complexes. Unbridged dimers are not found though they are strongly implicated as intermediates underlying carbonyl fluxionality.[3] For $Cp_2Ru_2(CO)_4$ an equilibrium between the bridged form and an unbridged isomer of unspecified structure is observed in solution,[3b,4a-c] though the solid-state structure is bridged.[4d] The corresponding Os complex is claimed to exist in an unspecified unbridged structure in the solid and solution.[4e] On the other hand we have the smaller class of $Cp_2M_2(CO)_4$ complexes with a d^5 configuration, M = Cr, Mo, W, in oxidation state I. The individual metal has a 15-electron count, a triple bond is indicated by the 18-electron rule, and indeed these metal–metal bonds are short: Cr–Cr, 2.22–2.28;[2c] Mo–Mo, 2.45[2b] Å. A pervasive structural feature of these compounds is the involvement of all the carbonyls in semibridging, i.e., in short, bonding approaches of carbonyls of one metal to those of the other.

The concept of metal–metal bonding, especially its extension to extremely strong and short multiple bonds, exemplified by the work of the Cotton group, forms a beautiful chapter of modern chemistry. The idea is heuristically useful and elegant. Yet in the case of bridged, supported metal centers the nagging doubt always remains as to the nature of the forces holding the two metals a certain distance apart and making for a low-spin ground-state configuration. This is especially so in the case of bridging carbonyls, where the bonding is highly delocalized, similar to that in diborane. We[5] and others[6] have argued that there is not much to be gained by imagining that there is a metal–metal bond in such carbonyl bridged complexes, and we would like to discuss the question again in the context of complexes **1** and **2**.

It may be indeed pleasing or even correct to assign a metal–metal bond order to a given compound of type **1** or **2**. But we view this as a description of nature and not as its understanding. Why do the d^7 $Cp_2M_2(CO)_4$ complexes all assume structural type **1** and the d^5 ones **2**? In principle geometries **1** and **2** (with or without semibridging), and even the unlikely looking **3**, are available to singly or triply bonded, d^7 or d^5, molecules. What makes a certain electron count opt for one structural type? That is the basic question, and if we can answer it we can say that we comprehend these molecules.

0002-7863/80/1502-2576$01.00/0

Setting Up

We will build up the orbitals of the structural alternatives **1–3** in order of increasing number of bridging carbonyls. This will be accomplished by a retrotheoretical analysis, in which $CpM(CO)_2$, CpM(CO), and CpM building blocks will be combined with each other and an increasing number of bridging ligands. The extended Hückel procedure, an approximate molecular orbital method, is used, with details provided in the Appendix.

The required orbitals are those of **4, 5, 6,** $CpM(CO)_n$, n = 0, 1, 2. One privileged coordinate system would place the z axis

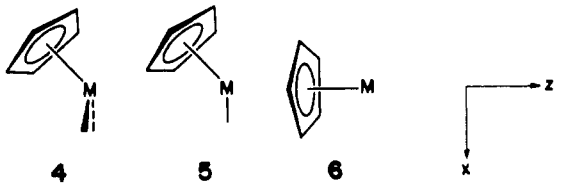

4 **5** **6**

along the metal to cyclopentadienyl normal, which would emphasize the natural descent of the fragments from a $CpM(CO)_3$ parent. Another coordinate system, however, will be chosen here. This prepares the fragment for its eventual incorporation in a metal–metal bonded dimer. To explore the characteristics of the metal–metal bond σ, π, and δ designations of pseudosymmetry around the M–M axis are useful. To prepare for this we will orient the z axis along the eventual direction of approach of the other metal atom.

The orbitals of all of these fragments have been discussed in the literature.[7] However we doubt that they are yet "a household word", so let us review them. The $CpM(CO)_n$ orbitals are related to those of $M(CO)_{n+3}$ by the isolobal replacement of a cyclopentadienyl by three carbonyls. The ML_n orbitals (**7–9**) are simple.[8] Above a nest of three levels, the

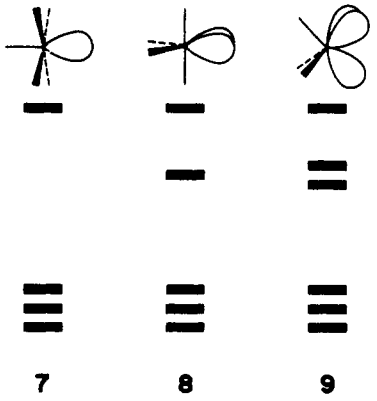

7 **8** **9**

remnants of the octahedral t_{2g}, there are disposed the delocalized equivalents of $6 - n$ hybrids pointing toward the missing octahedral sites.

On going to $CpM(CO)_n$, n = 1 or 2, the symmetry falls precipitously, to a single mirror plane. The electronic pseudosymmetry is also unbalanced, for a Cp unit lacks the acceptor characteristics of the three carbonyls it replaces. Nevertheless the gross features of the ML_n parent are discernible in the $CpM(CO)_n$ frontier orbitals. Each has a group of higher lying hybrids and a set of three t_{2g}-like orbitals below. The hybrids and t_{2g} sets are less well separated in the Mo case.

We are now ready for the construction of the various dimers.

The $Cp_2Cr_2(CO)_4$ Type—Four Semibridging Carbonyls

One would like to think that it is possible to unscramble the semibridging carbonyl interaction, i.e., one metal bonding to a carbonyl terminally connected to another metal, **10,** by first creating a situation where the M carbonyl and M′ are too far removed to interact, and then initiating a geometrical motion

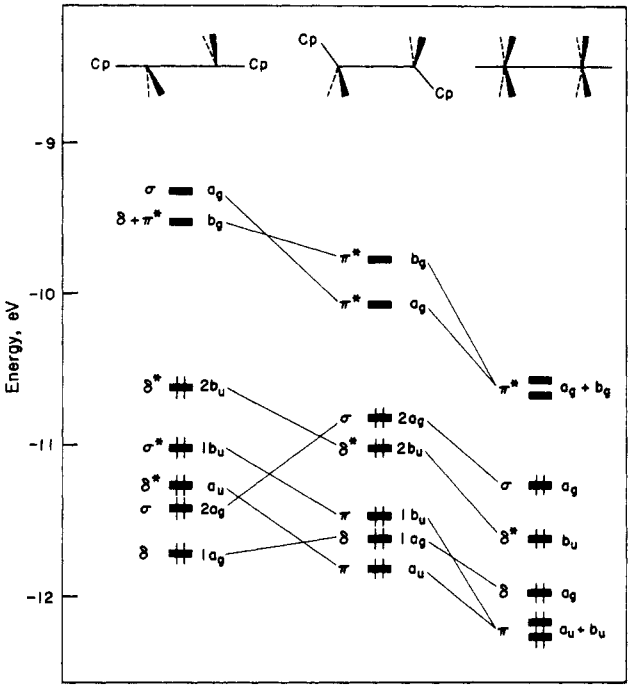

Figure 1. Frontier orbitals of $Cp_2Mo_2(CO)_4$ and $Mo_2(CO)_{10}^{2+}$. At left are the orbitals corresponding to the experimental geometry of $Cp_2Mo_2(CO)_4$ and in the middle those corresponding to an idealized octahedral geometry. The same MM distance (2.448 Å) is used in all the three structures.

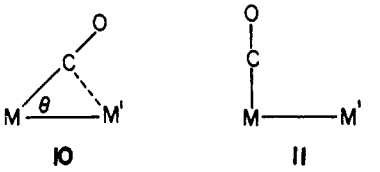

10 **11**

which would bring M′ and CO together. In practice this is difficult to do, but let us see what happens.

The observed structures have an M′–M–CO angle of 67–76°. Let us imagine that θ = 90° were a good model for no semibridging, and bring together two $CpM(CO)_2$ units in such a geometry, **12,** for a metal–metal separation of 2.448 Å, that

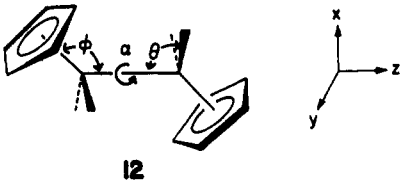

12

found in the Mo dimer. Here is the problem that arises. If θ is 90° and the Cp indeed takes the place of three carbonyls in an octahedral fragment (so that the M′–M–normal to Cp angle φ is 125.26°), then for most values of the torsion around the MM axis it is impossible to avoid unacceptable steric contacts. These occur either between the cyclopentadienyls or between a Cp and a carbonyl on the other metal. The most severe interactions are between Cp ring hydrogens near α = 0° (α is the torsion angle around the MM bond, α = 0° corresponding to eclipsed Cp's). Even if the Cp rings are rotated to create a cogwheel, H–H contacts as short as 1.8 Å remain at α = 0°. The result is a destabilization of that torsional region relative to large α—the "anti" orientation, α = 180°, actually depicted in **12** and related to the observed dimer structures, is some 32 kcal/mol more stable than the α = 0° rotamer. As we shall see, this number will be smaller for the iron case.

We now focus on the orbital pattern of the idealized "octahedral" dimer **12** at α = 180°. This is shown in the middle of Figure 1. This figure contains also at left the orbitals of the real

Table I. Composition of Frontier Orbitals of $Cp_2Mo_2(CO)_4$ in an Idealized Octahedral Fragment Geometry, $\theta = 90°$

orbital	type	energy, eV	% on metals	% composition of metal part
b_g	π^*	−9.80	44	$41yz + 2xy + 1y$
$3a_g$	π^*	−10.04 LUMO	52	$43xz + 6z^2 + 2(x^2 - y^2) + 1s$
$2a_g$	σ	−10.90 HOMO	64	$36z^2 + 18z + 3(x^2 - y^2) + 6s$
$2b_u$	δ^*	−11.03	56	$51(x^2 - y^2) + 4z^2 + 1x$
$1b_u$	π	−11.41	68	$61xz + 4z^2 + 3z + 1s$
$1a_g$	δ	−11.45	64	$43(x^2 - y^2) + 19z^2 + 2xz + 2x$
a_u	π	−11.58	71	$58yz + 10xy + 3y$

Table II. Structural Parameters for Idealized "Octahedral Fragment" and Observed $Cp_2M_2(CO)_4$

molecule	MM, Å	θ, deg	β, deg	ϕ, deg	ref
"octahedral fragment"	2.448	90	90	125.26	
$Cp_2Mo_2(CO)_4$	2.448	67.4	86.6	180	2b
$Cp_2Cr_2(CO)_4$	2.22	73.6	84.7	161.9	2c
$(C_5Me_5)_2Cr_2(CO)_4$	2.28	76.1	88.9	158.7	2a

geometry of $Cp_2Mo_2(CO)_4$ and at right the orbitals of a hypothetical decacarbonyl $Mo_2(CO)_{10}^{2+}$. We will return to these cogs in an explanation in a moment, but note immediately the five below two level pattern of the idealized and real geometries. A nice closed-shell structure is obtained for a d^5-d^5 electron count.

The filled levels in $Cp_2Mo_2(CO)_4$ at any α are two of a_g symmetry, two b_u, and one a_u. Table I summarizes their composition in the idealized geometry. The actual symmetry, C_{2h}, is so much lower than cylindrical that much mixing naturally occurs. The characterization of these orbitals as σ, π, or δ is to some extent arbitrary (for instance, the lowest a_u level is both π bonding and δ antibonding), but it is nevertheless a useful distinction based on predominant orbital type. It allows one to see explicitly the triple bond assigned to these molecules on the basis of electron-counting considerations. The occupied orbitals are of σ, π, π, δ, and δ^* type. These five orbitals contribute 0.620 of the 0.665 overlap population between the metal atoms, and that 0.620 partitions into 53% σ, 42% π, and 5% δ.

The five below two pattern is the most interesting aspect of the electronic structure of these molecules, for as we will see it differs significantly from the $Cp_2Fe_2(CO)_4$ geometries. At the same time it assures a low-spin ground state for the Cr, Mo, and W dimers. Where does that pattern come from? To answer that question we retreat in an isolobal replacement scheme, from **12** to an isoelectronic $Mo_2(CO)_{10}^{2+}$ (**13**). The orbitals

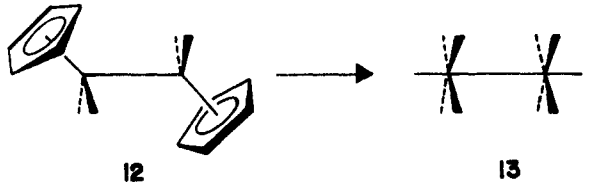

12 **13**

of this molecule, calculated at the same Mo–Mo separation of 2.448 Å as for **12**, are shown at right in Figure 2. The levels may be trivially constructed from those of two $M(CO)_5$ fragments, **7**, much as we and others have done for $Mn_2(CO)_{10}$.[8,9] There is a metal–metal σ bonding orbital and a total of six orbitals based on the t_{2g} set xy, xz, yz of each metal center. The symmetry of these is π, δ, δ^*, π^*. Their splitting, indicated in Figure 2, is quite substantial. This is a consequence of the good d orbital overlap at the relatively short Mo–Mo distance.

The five below two pattern is thus established already in the M_2L_{10} dimer and, as we shall shortly see, so is the incipient carbonyl bridging. The two orbitals that split away are of π^* symmetry. Now we return to the idealized $Cp_2Mo_2(CO)_4$ structure. Figure 2 shows the aforementioned splitting pattern and an expected movement to higher energy of *all* the orbitals. This is a consequence of replacing three good acceptors (carbonyls) by their electronic equivalent but a much poorer acceptor, a cyclopentadienyl. The symmetry is also greatly lowered by the substitution, which is responsible for the admixture of σ, π, and δ character exhibited in Table I.

To go from idealized octahedral fragment dimer **12** to the real semibridging geometry is a process that involves minimally a readjustment of three angles shown in **14**: the M′–M–CO angle θ defined earlier, the angle β between the carbonyls, and the angle ϕ between the MM axis and the normal to the Cp

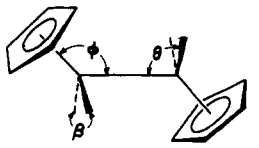

14

plane. These angles in the idealized structure and the two known crystal structures are summarized in Table II. The excursion in β is small, in θ also small but much more important because it gauges the semibridging, and the change in ϕ is very great.

We have explored several cuts through a potential-energy surface that connects the dimer made up of idealized octahedral fragments ($\theta = 90°$, $\beta = 90°$, $\phi = 125.26°$), with a realistic structure for the Mo case. The angular degrees of freedom are linked—for instance, it is costly to decrease θ unless the Cp rings on the other metal are moved out of the way through increasing ϕ. But the overall surface is in our calculations a soft one. Only 2 kcal/mol separate the idealized geometry from the real solid-state one—the two defined by the angles in the first two entries of Table I. Thus it is no surprise that the angle ϕ in the three structures known varies over a wide range.

The energy does not change much as all four carbonyls enter the semibridging region. And while there are changes in the individual d-block levels (center to left of Figure 1), the most dramatic effects occur in a theoretical descriptor of bonding, the Mulliken overlap populations—structures **15** and **16** show

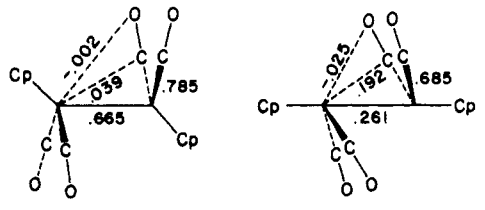

15 **16**

idealized real

the MM and the M–CO overlap populations in the geometries of the first two entries of Table II.

The MM overlap population in the real structure is much smaller than in the idealized one, for the same metal–metal separation. The M to semibridging or distal CO carbon overlap population, on the other hand, is much larger. All other overlap populations change less drastically, though in a well-defined pattern: in the real structure the M–terminally or directly bound C bond is weaker, as is the CO bond itself. The overlap

population between the metal and the oxygen of the distal CO goes from −0.002 to −0.025. The change is not great, but is especially significant because the metal-carbon bond is growing in strength in the course of the same deformation.

Along with these overlap population changes there is a shift of electron density, summarized in the charges of **17** and **18.**

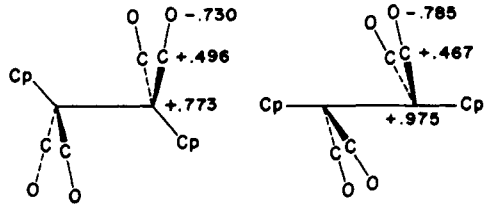

17 idealized **18** real

On going to the experimental geometry the metal atoms lose electron density to the carbonyls.

The electron redistribution attendant upon semibridging is entirely consistent with the replacement of metal-metal bonding by a metal-remote carbonyl interaction. More specifically that distal interaction involves occupied metal based orbitals acting as *donors* to carbonyl π^* *acceptor* orbitals.[10] The orbital details will be filled in momentarily, but the overall effect is indicated schematically in **19.** Note that the buildup

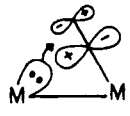

19

of M-distal CO bonding, diminution of M-direct CO and C-O bonding, the electron drift from metal to CO, all of these symptoms are consistent with the charge transfer being in the direction indicated. The M···O antibonding coupled with M···C bonding is a particularly striking sign.

Why is metal-metal bonding diminished as the semibridging interaction is turned on? The answer to this question is tied up with the details of the interaction schematically and incompletely indicated in **19.** The careful reader will have noted that in Figure 2 the a_u and $1b_u$ levels have changed designation on going from the idealized to the real structure, a_u from π to δ^*, $1b_u$ from π to σ^*. This is based upon their calculated composition. For instance, a_u in the idealized geometry was given in Table I as being made up of 71% on metal, 61% $\pi(yz$ and $y)$ and 10% $\delta^*(xy)$. In the real geometry the composition changes to 52% on metal, 5% π and 46% δ^*. A similar transformation occurs in $1b_u$, which goes from 68% on the metal, mostly π, in the idealized structure to 46% on the metal, predominantly σ^*.

These two orbitals are graphed in Figure 2. The greater part of what happens is a simple reorientation, shown in **20** and **21.**

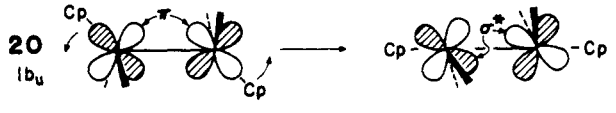

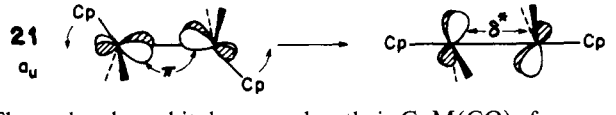

The molecular orbitals remember their $CpM(CO)_2$ fragment parentage and follow the fragment around as it reorients. The transformation of π character into δ^* and σ^* appears quite natural from this viewpoint.

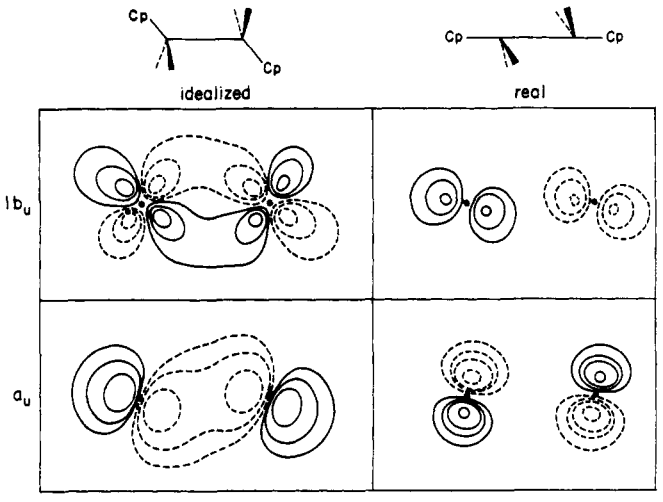

Figure 2. Contour diagrams of the occupied $1b_u$ and a_u orbitals of $Cp_2Mo_2(CO)_4$ showing only Mo contributions. The idealized octahedral geometry is on the left and the experimental geometry on the right. The $1b_u$ orbital is in the xz plane and the a_u orbital is in a plane parallel to xz and 0.5 Å in the y direction.

While this picture explains the loss of metal-metal bonding, it does not yet have the compensatory factor—metal carbonyl semibridging. To bring this into focus we must restore the carbonyl components omitted in **20** and **21** to these a_u and $1b_u$ orbitals. This is done in **22** and **23. 22** and **23** are drawn for the idealized octahedral fragment structure. A diminution of θ, i.e., a motion toward semibridging, the very same motion which

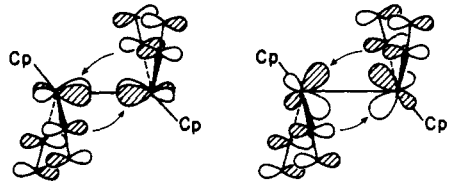

22 **23**

we claim demolishes metal-metal π bonding, that same distortion increases the metal to carbon (of semibridging carbonyl) interaction. This analysis is confirmed by an examination of the contributions to the metal to distal CO overlap populations orbital by orbital.

That the secondary interaction responsible for semibridging is a bonding one is a consequence of the way the phases of the M′ and the carbonyl on M in M′-M-CO are tied together. The COπ^* is tied to the d orbital on its own metal, M, through the primary back-bonding interaction. M is linked to M′ by metal-metal π bonding. This forces a bonding phase relationship between M and CO, which is increased upon the carbonyls bending over.

The phase relationship invoked and illustrated in **22** and **23** is present in the idealized dimer formed from octahedral fragments. It is enhanced in the real geometry, but the +0.039 overlap population is a definite sign of its existence in the octahedral dimer. But it can be traced back even further. Its roots are in the binuclear decacarbonyl $Mo_2(CO)_{10}^{2+}$, where orbitals analogous to **22** and **23,** namely, **24a,b,** are to be found. The M···C(O) overlap population in $Mo_2(CO)_{10}^{2+}$ is very

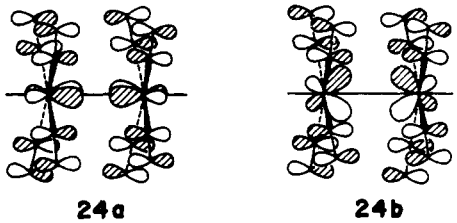

24a **24b**

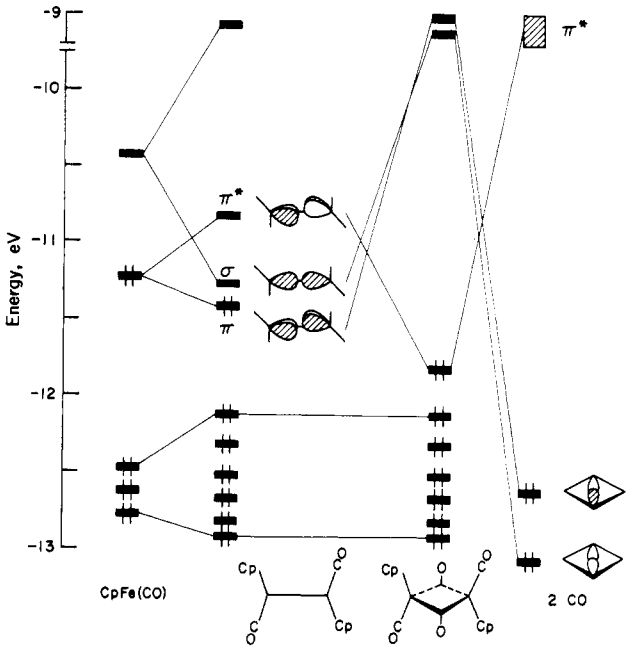

Figure 3. Interaction diagram for the formation of *trans*-$Cp_2Fe_2(CO)_2$ from two CpFeCO, and for *trans*-$Cp_2Fe_2(CO)_4$ from $Cp_2Fe_2(CO)_2$ and two CO's.

small, +0.009, but it is positive. Replacing three carbonyls by a Cp increases π bonding to the remaining two carbonyls and so primes the semibridging interaction.

By tracing the secondary interaction back to $M_2(CO)_{10}$ we have made a connection with an elegant explanation, already given by others in the literature,[11] of deformations of ML_4X, ML_5X, and M_2L_{10}.

Our conclusion on the d^5-d^5 structures is that the soft semibridging interaction in these is based on the donation of metal electrons to remote carbonyl π^* orbitals. It is inevitably accompanied by the loss of metal-metal π bonding. It must be clearly admitted that we do not as yet have a complete understanding of the electronic structure of these carbonyl systems. In particular we have not reasoned out why these semibridging carbonyls remain linear.

We will return to a brief discussion of the reactivity of these molecules at the end, but first let us examine the popular doubly bridged alternative.

Dibridged Complexes

Here we begin the building up of the orbitals of the isomeric dibridged geometries **1** by bringing together two CpM(CO) fragments. There is not much of a difference between the cis

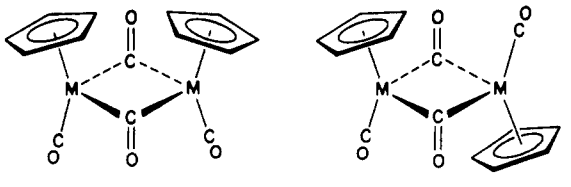

1 cis **1** trans

and trans alternatives, so only one of these is shown in Figure 3. These molecules have been studied theoretically before.[1d,12] A construction similar to ours has been employed by Hofmann in the analysis of $Cp_2Rh_2(CO)_2(CH_2)$ complexes.[7a,b]

Each component CpM(CO) unit has three low-lying orbitals and two higher hybrids. These combine to give a nest of six low-lying, mainly metal d combinations and three higher valence orbitals, which we have labeled π, σ, and π^* according to their bonding characteristics. (The actual symmetry is maximally C_{2v} or C_{2h}, depending on the isomer.) The fourth combination of the CpM(CO) hybrid levels, σ^* in symmetry, is too high to enter into further bonding interactions. It does, however, become the LUMO of the final composite molecule.

Now two carbonyls come in, at the right side of Figure 3. Their lone pair donor functions are of σ and π pseudosymmetry. These destabilize the hybrid combinations of matching symmetry. The remaining hybrid level, π^*, is in fact stabilized by interaction with carbonyl acceptor orbitals, as are several of the low-lying block of six orbitals.

The important feature of dibridged $Cp_2M_2(CO)_4$, and this is true of both cis and trans isomers, is that there are seven orbitals available for occupation. This is why this structural type is favored by d^7 complexes, i.e., M = Fe,Ru. The second hallmark of these compounds, the existence of separate cis and trans isomers, is also apparent from the construction. Suppose that the CpM(CO) units were brought together not in the observed geometries, but, say, 90° twisted around the MM axis away from there, as in **25.** Then the hybrid orbitals would not fall into a σ, π, π^* pattern but that shown schematically in **26**

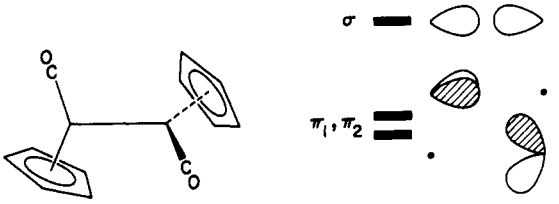

25 **26**

instead. π_1, π_2 here are hybrid combinations centered on each metal alone.

There is not much of an iron-iron bond in $Cp_2Fe_2(CO)_4$, no matter what 18-electron considerations say. This is most simply seen from Figure 3. The set of six t_{2g} orbitals is composed of bonding and antibonding combinations, equal in number. The seventh orbital is clearly metal-metal antibonding. Now s and p mixing into the lower t_{2g} d set builds in some σ-bonding character, as detailed in our discussion of d^{10}-d^{10} complexes,[13] but it is barely sufficient to overcome the π antibonding from the HOMO. The net Fe-Fe overlap population that we calculate is 0.03. Other molecular orbital calculations lead to a negative or small positive iron-iron bond order.[1d,12] Experimental determinations of difference densities from crystallographic studies indicate little or no electron density in between the irons.[1d]

Contributory evidence on the nature of the bonding in $[CpFe(CO)_2]_2$ is at hand in the crystal structures of $Cp_2Fe_2(CO)_2(Ph_2P(CH_2)_nPPh_2)^{0,+}$.[14] Apparently there is almost no effect on the Fe-Fe bond length upon oxidation. We could predict an actual contraction, since a π^* level is being vacated. (There is some disagreement between us and Sherwood and Hall,[12b] whose HOMO, like ours, is a_2, but is mainly δ^*.) A simplistic metal-metal single bonding picture presumably would predict elongation, as the σ bond is partially broken.

There is an intriguing if minor geometrical feature that characterizes the two different $Cp_2M_2(CO)_4$ isomers. In the trans structures the inner rhomboid is usually planar, while in the cis isomers it is slightly puckered, with a dihedral angle of δ = 164° between MCM planes being a typical value.[1]

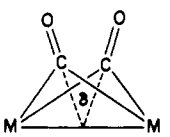

27

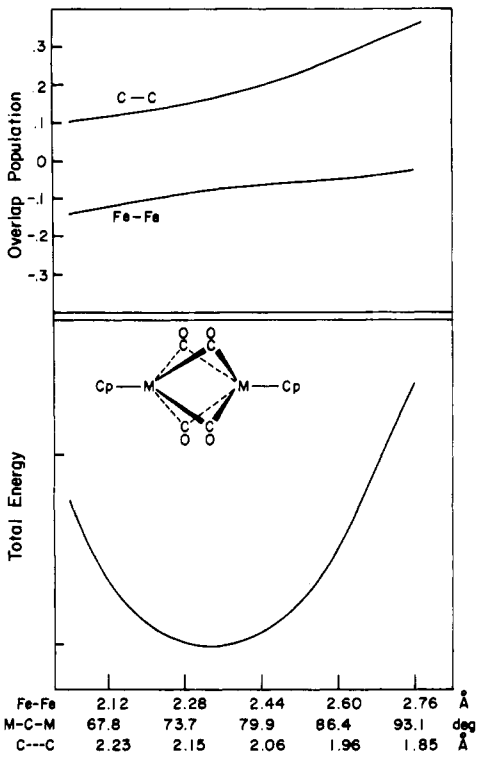

Figure 4. The lower part of the figure gives the changes in the total energy, scale markings 1 eV apart, with M-M distance in $CpFe(\mu\text{-}CO)_4FeCp$. Also plotted along the x axis are corresponding FeCFe angles and C···C nonbonded distances. The top part of the figure gives the variation in C-C and Fe-Fe overlap populations.

A Walsh diagram for the cis and trans isomers traces this effect to the π^* HOMO. It is shown schematically in **28** and

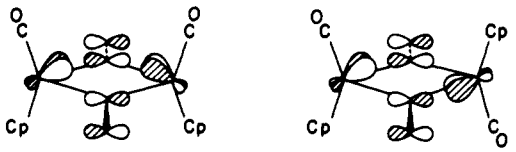

28 **29**

29. The tilt of the π^* orbital components reflects their CpM(CO) parentage.[7b] The puckering of the inner rhomboid in the cis isomer is a consequence of the bridging carbonyls moving so as to maximize their overlap with the metal orbitals. This requires them to rise above the plane, toward the terminal CO's and away from the Cp's, as observed experimentally. We calculate a shallow minimum at a puckering angle δ of 170°. In the trans structure a flapping in either direction increases carbonyl interaction with one orbital and decreases it with the other. There is no net gain; the ring remains planar. The analysis here is similar to that given earlier for ring puckering or the absence thereof for $L_nM(\mu\text{-}CO)_2ML_n$.[15]

Before we return to a comparison of the semibridging and doubly bridging structures we must consider another alternative.

Four Bridging Carbonyls

The quadruply bridged dimer structure, **3**, for $Cp_2M_2(CO)_4$ might at first sight seem outlandish. But there are several

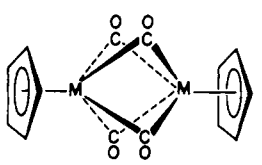

3

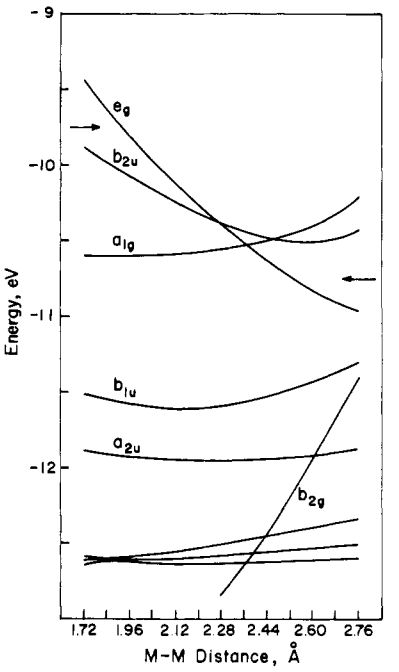

Figure 5. Walsh diagram for M-M stretch in $CpMo(\mu\text{-}CO)_4MoCp$. Arrow indicates the level of electron occupancy.

complexes with four ligands bridging through a single atom, not to speak of the multitude of complexes with four polyatomic bridges of the acetate or diazenido type. For instance, there is the agnohydride $(PR_3)_2H_2Re(\mu\text{-}H)_4Re(PR_3)_2H_2$, whose structure was recently settled,[16] and the SR bridging $(toluene)Mo(\mu\text{-}SMe)_4Mo(toluene)^{2+}$ [17] and $CpMo(\mu\text{-}SMe)_4MoCp^{0,+}$ [18]

The basic problem of all structures containing four or more monoatomic bridges X is that for a realistic MX distance the set of MM distances (or MXM or XMX angles) that gives a reasonable XX contact, that prevents the bridging groups from bumping into each other, is highly constrained. The scale of Figure 4, for instance, shows the combination of geometrical parameters that is forced for a hypothetical quadruply bridged $CpFe(\mu\text{-}CO)_4FeCp$ by a typical Fe-C distance of 1.90 Å. To keep the bridging carbonyl carbons more than 2.0 Å apart the Fe-Fe distance must be less than 2.55 Å. The actual computed minimum is for a still shorter iron separation.

The bonding in these complexes may be built up in the following way. Two MCp units combine to give a nest of six low-lying t_{2g}-type levels and $\pi(e_u)$, $\pi^*(e_g)$, $\sigma(a_{1g})$, and $\sigma^*(a_{2u})$ combinations from the hybrids. The last, σ^*, is too high to interact effectively. The four carbonyls introduce another local symmetry, D_{4h}, and that pseudosymmetry appears to dominate over the D_{5d} or D_{5h} symmetry of CpMMCp. The carbonyl lone pair combinations, a_{1g}, e_u, and b_{1g} in symmetry, interact with the CpMMCp levels to give nine lower levels: five surviving t_{2g}-type orbitals and four orbitals derived from the carbonyl lone pairs but now to be thought of as giving the M-(μ-CO)-M bonding. Above these is a degenerate pair, e_g, derived from CpMMCp π^* with some μ-CO π^* mixing, metal-metal antibonding.

The e_g orbital pair is occupied in the Fe case and empty for Cr. In neither case is there much of a metal-metal bond, for the six t_{2g} levels are approximately nonbonding, and the e_g is metal-metal π antibonding. Figure 5 indicates the Fe-Fe overlap population as a function of separation. It is negative. The metal-metal bonding, or better said lack thereof, resembles that in $Fe_2(CO)_9$.[5b,d,6c]

An intriguing feature of these calculations, noted in Figure 4, is the presence of substantial positive overlap populations

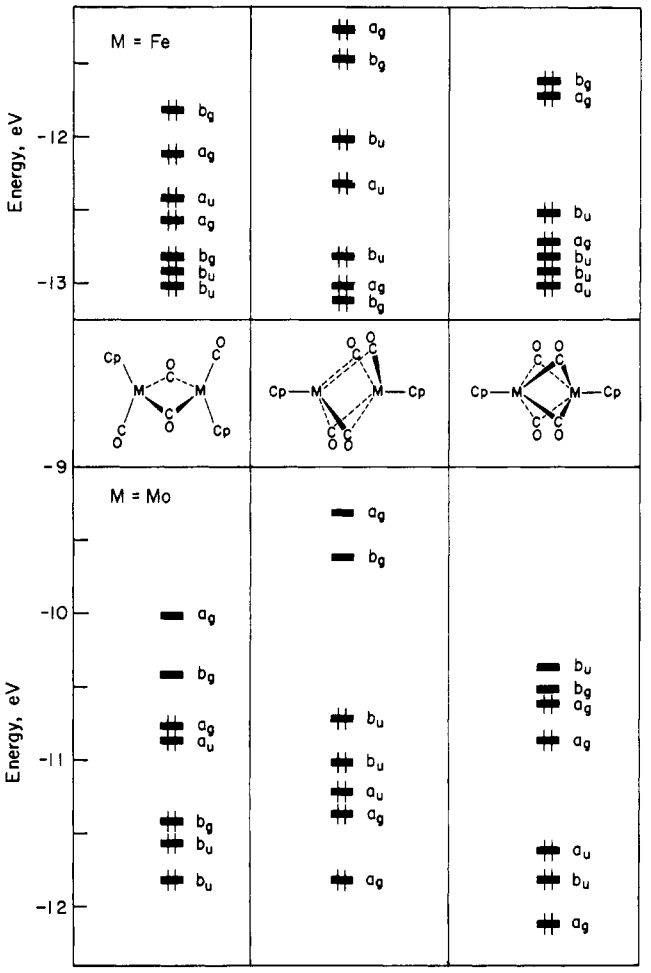

Figure 6. Comparison of the frontier orbitals of the three basic structures of $Cp_2M_2(CO)_4$ complexes. The top part gives the levels for Fe and the bottom for Mo.

between the carbons of the bridging carbonyls. These are in the range of partial bonding interactions, and they only *increase* when the geometrical constraints of the bridge force the carbonyls together. On looking back at our previous calculations on the $Re(\mu\text{-}H)_4Re$ dimers[4c] we also find a similar effect. The origin of this phenomenon and its connection to eliminations of bridging atoms will be discussed in a separate paper; here we note only the existence of the effect.

From the substantial gap between the lower levels and the $e_g\pi^*$ level one would have expected a nice closed-shell structure, e_g empty, for the analogous tetrabridged molybdenum analogue, d^5-d^5. This does not turn out to be so. Figure 5 shows the computed energy levels for symmetrically tetrabridged $CpMo(\mu\text{-}CO)_4MoCp$. The π^*e_g level is there, but near it are two other levels, of a_{1g} and b_{2u} pseudosymmetry. These have come from the d block, derived from the $2a_g$ and $2b_u$ levels that we have discussed earlier in the section on semibridged complexes. The reason for the difference between Fe and Mo, i.e., why these d block levels are near the hybrid π^* combination in Mo but not Fe, is to be found in the spatial extent of the orbitals and the relative energy of d and s,p orbitals—it is what is behind the different splitting of the hybrid set from the "t_{2g}" set in the fragments themselves.

The reason that this level pattern, which persists for the entire range of metal-metal separations plotted, is important is that it creates an instability for the quadruply bridging Mo structure. For iron one had a closed-shell structure and a reasonable, if high-energy, alternative for the $[CpFe(CO)_2]_2$ structure. For molybdenum we have what extended Hückel numbers indicate is an energetically good structure, but it has a near degeneracy— four electrons to put into the high-lying four levels of Figure 5. Either a high-spin complex or a second-order Jahn-Teller distortion to another geometry (the semibridging one?) is likely.

Structural Alternatives

Each of the geometrical alternatives has been considered separately—it is now appropriate to intercompare them. Figure 6 puts on one graph the energy levels of the quadruply semibridged **2**, the dibridged **1** (the cis isomer, for convenience, the trans isomer not being very different), and the quadruply bridged **3.** There are two parts to the figure, showing the level patterns for parameters and distances appropriate to iron and molybdenum. The purpose of the repetition is to point up the similarities (for **1** and **2**) and differences (for **3**, discussed in the last section).

For the quadruply semibridging geometry **2** there is the already explained pattern of five below two. The same obtains for **3** in the case of iron but not molybdenum. For **1** all seven labels are bunched together. Looking simplistically for substantial gaps between filled and unfilled levels, we would conclude that all structures are in principle available for d^7-d^7 But only **2** provides a low-spin alternative and some (as we will see, not much) freedom from kinetic reactivity toward bases for the d^5-d^5 molecules.

What about the interconversions of the various structures? Experimentally the situation is unambiguous for the d^7-d^7 case, M = Fe. The elegant experimental studies of Cotton, Adams, Gansow, and co-workers show clearly that the isomeric structures **1**-*cis* and -*trans* interconvert and scramble carbonyls not through the quadruply bridging structure **3**, but by opening up both bridges and rotating about the metal-metal bond.[3] As far as we are aware nothing is known about rotation or carbonyl interchange in the quadruply semibridging d^5-d^5 complexes.[19] Let us see what can be said theoretically about these interconversions.

The symmetry of the structures and interconversion waypoints is relatively high, allowing the construction of level correlation diagrams. One can move from **1**-*cis* or -*trans* to **3** preserving a twofold symmetry axis—perhaps the swinging of the terminal carbonyls into bridging sites is easiest envisaged for the trans isomer of **1.** The interconversion of **2** and **3** also maintains a twofold axis, but an even higher pseudosymmetry, C_{2h}, is really there. Transforming either isomer of **1** into **2** is a more complex motion, since a simple opening of the two bridges leads not into **1** but into a rotamer, one in which the carbonyls are also removed from semibridging.

For the d^7-d^7 system a correlation diagram shows that moving two carbonyls into bridge sites, i.e., a transformation to quadruply bridging **3**, is symmetry allowed. But so is opening up the two bridges to reach a single bonded, but not semibridging, structure **30.** (No conformational information is as yet implied in **30**.) We thus have a competition between two

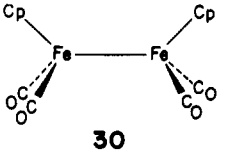

30

symmetry-allowed processes. Though our calculations actually favor the breaking of bridges in **1** rather than the making of more of them, one cannot trust extended Hückel calculations for these energetics. It is better to rely on experiment, and the experimental answer, mentioned above, is crystal clear—the process occurs by breaking bridges.[3]

Given that it is an allowed process to break the bridges we must inquire about the rotational barrier around the Fe-Fe bond in **30,** for it must be low enough to allow rotation between the entrance and exit channels correspondingly leading from

and to the bridged isomers. In examining this rotation we face an uncertainty in our lack of knowledge of the metal-metal bond length and Cp and CO bending angles. We have somewhat arbitrarily left the angle φ between the Cp normal and the Fe-Fe bond at its value of 137° in a model for **1**, taken the M-M-CO angles θ at 90° (see structure **12** for a definition of these parameters), and varied the torsion α (α = 0° means Cp rings eclipsed) for two Fe-Fe distances, 2.5 and 2.7 Å. Figure 7 shows the individual energy levels and total energy as a function of α. The Fe-Fe distance is here 2.7 Å, stretched by some 0.2 Å from that distance in the normal dibridged structures.

The computed barrier is small, 4 kcal/mol. At the shorter Fe-Fe distance of 2.5 Å the curve has a similar shape, but with a larger hill at α = 0°, of 10 kcal/mol. Either number is consistent with the experimental results of a low barrier.

The shape of the barrier is amusing. There are minima at α = 60 and 180°, "gauche" and "anti". This is reminiscent of a butane—a Fourier decomposition would lead to V_1 and V_3 components. Short CO-CO contacts may be responsible for the V_1 maximum at α = 0°. The behavior of the individual levels with θ is interesting, and can be analyzed in substantial detail. Here we point only to the five below two pattern at α = 180°, the point corresponding to the quadruply semibridging structures.

Now let us go back to the d^5-d^5 structures. Transformations to dibridged **1** and quadruply bridged **3** are not forbidden, but for Mo both would be in our calculations open-shell structures, subject to second-order Jahn-Teller distortions. So going by the requirement for a substantial gap between filled and unfilled levels we would not expect an easy deformation to **1** or **3.** Interestingly the torsion about the Mo-Mo bond (after tilting the carbonyls out of semibridging) is a forbidden reaction. This may be seen from Figure 7 by populating the lowest five levels. So the torsion should be a difficult process.

In the Mo case we encounter a typical failure of the extended Hückel total energy as a criterion for evaluating thermodynamic stabilities. While for iron the isomeric relationships were correctly reproduced (the dibridged isomer was lowest in energy), for Mo both the dibridged and the quadruply bridged structural alternatives are computed to be more stable than the correct semibridged structure. The total energy cannot be trusted but we are certain that the energetic trends with angular variations are reliable.

A more detailed discussion of $[CpM(CO)_n]_2$, n = 1, 2, isomerizations will be given elsewhere by Hofmann.[20] The reader is also referred to a forthcoming exhaustive analysis of when M_2L_{10} complexes will bridge.[21]

Reactivity of the d^5-d^5 Complexes

The $Cp_2M_2(CO)_4$ complexes with M = Cr, Mo, and W have a rich chemistry, growing rapidly through the researches of Curtis, Chisholm, Cotton, Wrighton, and their co-workers.[2] The chemistry is characterized by coordinative unsaturation, the addition of one or two ligands such as CO, acetylene, allene etc., acting as Lewis bases. The products of adding two carbon monoxides are the fascinating $Cp_2M_2(CO)_6$, M = Cr, Mo, W. These have long and weak metal-metal bonds, for instance, 3.235 Å for Mo,[19] 3.222 Å for W,[19] and 3.281 Å for Cr[23] (3.343 Å in a phosphite derivative[24]), a hint of a high-spin-low-spin equilibrium that may be coupled to a reversible metal-metal bond cleavage,[23,24] and a fascinating chemistry.[2,22-26] The carbonyls, as constrained as they are in these molecules, are not semibridging.[19,23,24]

While it is attractive to associate coordinative unsaturation with multiple bonding, the connection is not all that clear. All that is required, in molecular orbital language, is the presence in the substrate of a seat of electrophilic activity, a good acceptor orbital. We do not find much of a triple bond in the

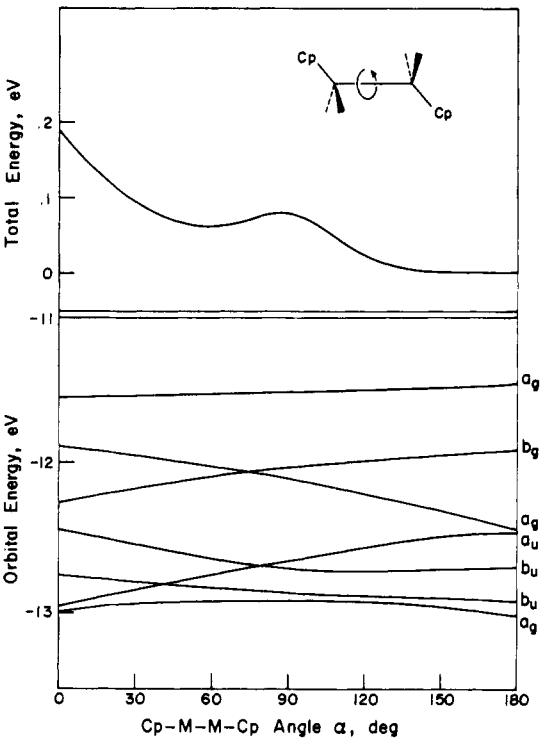

Figure 7. Rotation barrier along Fe-Fe axis in $Cp_2Fe_2(CO)_4$ using the idealized octahedral geometry above and the corresponding Walsh diagram below. Fe-Fe distance = 2.7 Å.

d^5-d^5 complexes, but we do have two nice low-lying orbitals, a_g and b_g in Figure 1.

These acceptor levels are shown in **31** and **32.** Their descent from π^* levels of $Mn_2(CO)_{10}$ is quite clear. The substitution

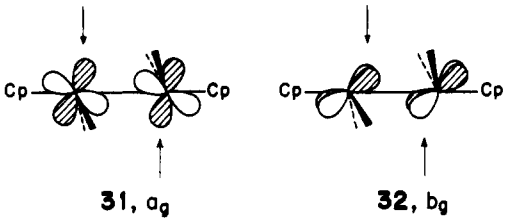

31, a_g **32**, b_g

of three CO's by Cp and the geometrical distortions mix in some σ character in a_g and δ in b_g, which is apparent from the tilt.

Both a_g and b_g have substantial density in the more or less open part of the molecule. This is not indicated as well in the schematic **31, 32** as it is in a contour map of the orbitals, Figure 8. This density should be available to donors in certain specific ways. For instance, a single donor should come in along the direction of an arrow in **31** or **32.** Such reactions occur, but they seem to do so from the other side, placing the MM bond trans to the incoming ligand. We cannot account for these observations from our theoretical model. In general, addition of one or two bases appears to be accompanied by disruption of the carbonyl semibridging.[2,22]

We would expect that acetylenes would interact initially from one side of the molecule. This does not use the full acceptor capability of the binuclear fragment, and that cannot be used unless one $CpM(CO)_2$ group rotates. This disrupts semibridging but allows a "tetrahedral" coordination of the acetylene. In all the structures with acetylenes, allenes, or $NCNMe_2$ one semibridging interaction on the other side of the molecule is maintained.[2d]

The choice that molecules make between bridged and unbridged structures is a delicate one, depending on small increments in bonding. Yet it is a pervasive feature of inorganic

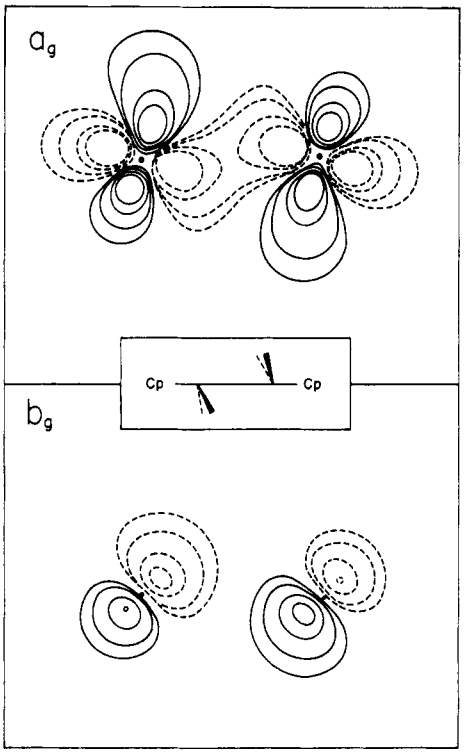

Figure 8. Contour diagrams of the two LUMOs of $Cp_2Mo_2(CO)_4$ in the experimental geometry. The a_g orbital is in the xz plane and the b_g orbital is in a plane parallel to xz and 0.5 Å in the y direction.

chemistry. This paper is only a beginning—we intend to find out why some molecules bridge and why some others do not.

Acknowledgment. We are grateful to S. Shaik for valuable discussions and to M. D. Curtis for perceptive critical comments and experimental information. Our research was supported by the National Science Foundation through Research Grant CHE 782 8048 and NSF MSC Grant DMR-7681083 to the Materials Science Cenfer at Cornell University.

Appendix

All calculations were of the extended Hückel type,[27] with H_{ii}'s and orbital exponents taken from previous work.[28] Relative energies of the orbitals of the idealized octahedral $CpM(CO)_n$ fragments (n = 0, 1, 2; M = Mo, Fe) were calculated using the same geometry for Fe and Mo, with the following parameters: C-H = 1.08, C-M = 2.21, C-C = 1.41, M-CO = 1.8, C-O = 1.15 Å. Energy levels for the observed $Cp_2Mo_2(CO)_4$ structure in Figure 1 were calculated using the experimental geometry but with a linear M-C-O (left column of Figure 1). The idealized octahedral geometry has the same bond distances as in the experimentally observed geometry (middle column). The hypothetical D_{4h} $Mo_2(CO)_{10}^{2+}$, at right, has Mo-Mo = 2.448, Mo-C = 2.1, and C-O = 1.155 Å. The geometry of *trans*-$Cp_2Fe_2(CO)_4$ was adapted from its X-ray structure, and the fragments used in Figure 3 shared the same geometrical parameters. The tetrabridging structures have D_{4h} symmetry at the bridging center with M-CO = 1.90 Å. Other geometrical parameters for $CpMo(\mu\text{-}CO)_4MoCp$ were C-H = 1.09 C-C = 1.42, C-Mo = 2.21, C-O = 1.155 Å, and for $CpFe(\mu\text{-}CO)_4FeCp$ were C-H = 1.08, C-C = 1.40, C-Fe = 2.11, C-O = 1.19 Å.

References and Notes

(1) (a) Piper, T. S.; Cotton, F. A.; Wilkinson, G. *J. Inorg. Nucl. Chem.* **1955,** 165–174. Cotton, F. A.; Liehr, A. D.; Wilkinson G. *Ibid.* **1955,** *1,* 175–186. Cotton, F. A.; Stammreich, H.; Wilkinson, G. *Ibid.* **1959,** *9,* 3–7. (b) Mills, O. S. *Acta Crystallogr.* **1958,** *11,* 620–623. Bryan, R. F.; Green, P. T. *J. Chem. Soc. A* **1970,** 3064–3068. (c) Bryan, R. F.; Green, P. T.; Field, D. S.; Newlands, M. J. *Chem. Commun.* **1969,** 1477. *J. Chem. Soc. A* **1970,** 3068–3074. (d) Mitschler, A.; Rees, B.; Lehmann, M. S. *J. Am. Chem. Soc.* **1978,** *100,* 3390–3397. (e) Nelson, N. J.; Kime, N. E.; Shriver, D. F. *Ibid.* **1969,** *91,* 5173–5174. Kim, N. E.; Nelson, N. J.; Shriver, D. F. *Inorg. Chim. Acta* **1973,** *7,* 393–396. (f) McArdle, P.; Manning, A. G.; Stevens, F. S. *Chem. Commun.* **1969,** 1310–1311. Stephens, F. S. *J. Chem. Soc. A* **1970,** 1722–1725. (g) Carty, A. J.; Ng, T. W.; Carter, W.; Palenik, G. J.; Birchall, T. *Chem. Commun.* **1969,** 1101–1102. (h) Huttner, G.; Gartzke, W. *Chem. Ber.* **1974,** *107,* 3786–3799. (i) Kirchner, R. M.; Ibers, J. A. *J. Organomet. Chem.* **1974,** *82,* 243–255. (j) Joshi, K. K.; Mills. O. S.; Pauson, P. L.; Shaw, B. W.; Stubbs, W. H. *Chem. Commun.* **1965,** 181–182. (k) Weaver, J.; Woodward, P. *J. Chem. Soc., Dalton Trans.* **1973,** 1439–1443. (l) English, R. B.; Haines, R. J.; Nassimbeni, L. R. *J. Organomet. Chem.* **1977** *135,* 351–360. English, R. B.; Nassimbeni, L. R.; Philpott, M. F. *Acta Crystallogr., Sect. B* **1978,** *34,* 2304–2306. (m) Greene, P. T.; Bryan, R. F. *Inorg. Chem.* **1970,** *9,* 1464–1471. (n) Campbell, I. L. C.; Stephens, F. S. *J. Chem. Soc., Dalton Trans.* **1975,** 982–985. (o) Cotton, F. A.; Frenz, B. A.; Troup, J. M.; Deganello, G. *J. Organomet. Chem.* **1973,** *59,* 317–327. (p) Adams, R. D.; Cotton, F. A.; Troup, J. M. *Inorg. Chem.* **1974,** *13,* 257–261. (q) Adams, R. D.; Brice, M. D.; Cotton, F. A. *Ibid.* **1974,** *13,* 1080–1085. (r) Cotton, F. A.; Frenz, B. A.; White, A. J. *Ibid.* **1974,** *13,* 1407–1411. (s) Churchill, M. R.; Kalra, K. L. *Inorg. Chem.* **1973,** *12,* 1650–1656. (t) Kirchner, R. M.; Marks, T. J.; Kristoff, J. S.; Ibers, J. A. *J. Am. Chem. Soc.* **1973,** *95,* 6602–6613. (u) Bailey, N. A.; Radfor, S. L.; Sanderson, J. A.; Tabatabaian, K.; White, C.; Worthington, J. M. *J. Organomet. Chem.* **1978,** *154,* 343–351. (v) Burlitch, J. M.; Burk, J. H.; Leonowicz, M. E.; Hughes, R. E. *Inorg. Chem.* **1979,** *18,* 1702–1709. (w) Bennett, M. J.; Brooks, W.; Elder, M.; Graham, W. A. G.; Hall, D.; Kummer, R. *J. Am. Chem. Soc.* **1970,** *92,* 208–209. (x) Chan, L. Y.; Einstein, F. W. B. *Acta Crystallogr., Sect. B* **1970,** *26,* 1899–105.

(2) (a) Potenza, J.; Giordano, P.; Mastropaolo, D.; Efraty, A.; King, R. B. *J. Chem. Soc., Chem. Commun.* **1972,** 1333–1334. Potenza, J.; Giordano, P.; Mastropaolo, D.; Efraty, A. *Inorg. Chem.* **1974,** *13,* 2540–2544. King, R. B.; Bisnette, M. B. *J. Organomet. Chem.* **1967,** *8,* 287–297. King, R. B.; Efraty, A. *J. Am. Chem. Soc.* **1971,** *93,* 4950–4952; **1972,** *94,* 3773–3779. King, R. B.; Iqbal, M. Z.; King, A. D., Jr. *J. Organomet. Chem.* **1979,** *171,* 53–63. (b) Klingler, R. J.; Butler, W. M.; Curtis, M. D. *J. Am. Chem. Soc.* **1978,** *100,* 5034–5039; **1975,** *97,* 3535–3536. (c) Curtis, M. D.; Butler, W. M. *J. Organomet. Chem.* **1978,** *155,* 131–145. (d) Chisholm, M. H.; Rankel, L. A.; Bailey, W. I., Jr.; Cotton, F. A.; Murillo, C. A. *J. Am. Chem. Soc.* **1977,** *99,* 1261–1262. Bailey, W. I., Jr.; Chisholm, M. H.; Cotton, F. A.; Murillo, C. A.; Rankel, L. A. *Ibid.* **1978,** *100,* 802–807. Chisholm, M. H.; Cotton, F. A.; Extine, M. W.; Rankel, L. A. *Ibid.* **1978,** *100,* 807–811. Bailey, W. I., Jr.; Cotton, F. A.; Jamerson, J. D.; Kolb, J. B. *J. Organomet. Chem.* **1976,** *121,* C23–C26. Bailey, W. I., Jr.; Collins, D. M.; Cotton, F. A. *Ibid.* **1977,** *135,* C53–C56. Bailey, W. I., Jr.; Chisholm, M. H.; Cotton, F. A.; Rankel, L. A. *J. Am. Chem. Soc.* **1978,** *100,* 5764–5773. (e) Ginley, D. S.; Wrighton, M. S. *J. Am. Chem. Soc.* **1975,** *97,* 3533–3535. Ginley, D. S.; Bock, C. R.; Wrighton, M. S. *Inorg. Chim. Acta* **1977,** *23,* 85–94. Ginley, D. S.; Bock, C. R.; Wrighton, M. S.; Fischer, B.; Tipton, D. L.; Bau, R. *J. Organomet. Chem.* **1978,** *157,* 41–50.

(3) (a) Bullit, J. G.; Cotton, F. A.; Marks, T. J. *J. Am. Chem. Soc.* **1970,** *92,* 2155–2156. *Inorg. Chem.* **1972,** *11,* 671–676. (b) Gansow, O. A.; Burke, A. R.; Vernon, W. D. *J. Am. Chem. Soc.* **1972,** *94,* 2550–2552; **1976,** *98,* 5817–5826. (c) Harris, D. C.; Rosenberg, E.; Roberts, J. D. *J. Chem. Soc., Dalton Trans.* **1974,** 2398–2403. (d) Adams, R. D.; Cotton, F. A. *Inorg. Chim. Acta* **1973,** *7,* 153–156. Cotton, F. A. *Bull Soc. Chim. Fr.* **1973,** 2588–2592. Adams, R. D.; Cotton, F. A. *J. Am. Chem. Soc.* **1973,** *95,* 6589–6594. Adams, R. D.; Brice, M. D.; Cotton, F. A. *Ibid.* **1973,** *95,* 6594–6602. Adams, R. D.; Cotton, F. A. *Inorg. Chem.* **1974,** *13,* 249–253. Cotton, F. A.; Frenz, B. A. *Ibid.* **1974,** *13,* 253–256. Cotton, F. A.; Kruczynski, L.; White, A. J. *Ibid.* **1974,** *13,* 1402–1407. References 1p,q. (e) Adams, R. D.; Cotton, F. A. In "Dynamic Nuclear Magnetic Resonance Spectroscopy", Jackman, L. M., Cotton, F. A., Eds.; Academic Press: New York, 1975; Chapter 12.

(4) (a) Fischer, R. D.; Vogler, A.; Noack, K. *J. Organomet. Chem.* **1967,** *7,* 135–149. (b) Noack, K. *Ibid.* **1967,** *7,* 151–156. (c) McArdle, P.; Manning, A. R. *J. Chem. Soc. A* **1970,** 2128–2132. (d) Mills, O. S.; Nice, J. P. *J. Organomet. Chem.* **1967,** *9,* 339–344. (e) Reference 6 in ref 4a.

(5) (a) Summerville, R. H.; Hoffmann, R. *J. Am. Chem. Soc.* **1976,** *98,* 7240–7254. (b) Lauher, J. W.; Elian, M.; Summerville, R. H.; Hoffmann, R. *Ibid.* **1976,** *98,* 3219–3224. (c) Dedieu, A.; Albright, T. A.; Hoffmann, R. *Ibid.* **1979,** *101,* 3141–3151. (d) Summerville, R. H.; Hoffmann, R. *Ibid.* **1979,** *101,* 3821–3831.

(6) See, for instance, (a) Mason, R.; Mingos, D. M. P. *J. Organomet. Chem.* **1973,** *50,* 53–61. (b) Lewis, J. *Pure Appl. Chem.* **1965,** *10,* 11–36. (c) References 19 and 20 in Teo, B. K.; Hall, M. B.; Fenske, R. F.; Dahl, L. F. *Inorg. Chem.* **1975,** *14,* 3103–3117.

(7) (a) $CpM(CO)_2$: Hofmann, P. *Angew. Chem.* **1977,** *89,* 551–553. Habilitationsschrift, Universität Erlangen, 1977. Green, J. C.; Jackson, S. E. *J. Chem. Soc., Dalton Trans.* **1976,** 1698–1702. Lichtenberger, D. L.; Fenske, R. F. *J. Organomet. Chem.* **1976,** *117,* 253–264. Schilling, B. E. R.; Hoffmann, R.; Lichtenberger, D. L. *J. Am. Chem. Soc.* **1979,** *101,* 585–591. (b) CpM(CO): Hofmann, P. *Angew. Chem.* **1979,** *91,* 591–593. (c) CpM: Elian, M.; Chen, M. M.-L.; Mingos, D. M. P.; Hoffmann, R. *Inorg. Chem.* **1976,** *15,* 1148–1155, and references cited therein.

(8) (a) Elian, M.; Hoffmann, R. *Inorg. Chem.* **1975,** *14,* 1058–1076. (b) Burdett, J. K. *J. Chem. Soc., Faraday Trans. 2* **1974,** *70,* 1599–1613. (c) Mingos, D. M. P. *J. Chem. Soc., Dalton Trans.* **1977,** 602–610. *Adv. Organomet. Chem.* **1977,** *15,* 1–51.

(9) (a) Brown, D. A.; Chambers, W. J.; Fitzpatrick, N. J.; Rawlinson, R. M. *J Chem. Soc. A* **1971,** 720–725. (b) Hall, M. B. *J. Am. Chem. Soc.* **1975,** *97,* 2057–2065. (c) Shustorovich, E. M.; Korol'kov, D. V. *Zh. Strukt. Khim.* **1972,** *13,* 682–688. Shustorovich, E. M. "The Chemical Bond"; Nauka: Moscow, 1973. (d) Korol'kov, D. V.; Miessner, H. *Z. Phys. Chem. (Leipzig)* **1973,** *253,* 25–32. Miessner, H.; Korol'kov, D. V. *Zh. Strukt. Khim.* **1972,** *13,* 689–700. (e) Levenson, R. A.; Gray, H. B. *J. Am. Chem. Soc.* **1975,**

97, 6042-6051.
(10) This is consistent with Cotton's original suggestion of the electronic character of semibridging interactions: Cotton, F. A. *Prog. Inorg. Chem.* **1976**, *21*, 1-28.
(11) (a) Berry, A. D.; Corey, F. R.; Hagen, A. P.; MacDiarmid, A. G.; Saalfeld, F. E.; Wayland, B. B. *J. Am. Chem. Soc.* **1970**, *92*, 1940-1945. (b) Reference 8a.
(12) (a) Bénard, M. *J. Am. Chem. Soc.* **1978**, *100*, 7740-7742. *Inorg. Chem.* **1979**, *18*, 2782-2785. (b) Sherwood, D. E., Jr.; Hall, M. B. *Ibid.* **1978**, *17*, 3397-3401.
(13) (a) Dedieu, A.; Hoffmann, R. *J. Am. Chem. Soc.* **1978**, *100*, 2074-2079. (b) Mehrotra, P. K.; Hoffmann, R. *Inorg. Chem.* **1978**, *17*, 2187-2189.
(14) (a) Haines, R. J.; duPreez, A. L. *J. Organomet. Chem.* **1970**, *21*, 181-193. *Inorg. Chem.* **1972**, *11*, 330-336. (b) Hardcastle, K.; Mason, R., cited in ref 7 of ref 12b.
(15) Pinhas, A. R.; Hoffmann, R. *Inorg. Chem.* **1979**, *18*, 654-658.
(16) Bau, R.; Carroll, W. E.; Teller, R. G.; Koetzle, T. F. *J. Am. Chem. Soc.* **1977**, *99*, 3872-3874.
(17) Silverthorn, W. E.; Couldwell, C.; Prout, K. *J. Chem. Soc., Chem. Commun.* **1978**, 1009-1011.
(18) Connelly, N. G.; Dahl, L. F. *J. Am. Chem. Soc.* **1970**, *92*, 7472-7474.
(19) Something is known about internal rotation in the related d^5-d^5 single bonded $[CpM(CO)_3]_2$ complexes: Adams, R. D.; Collins, D. M.; Cotton, F. A. *Inorg. Chem.* **1974**, *13*, 1086-1090.
(20) Hofmann, P., to be published.
(21) Shaik, S.; Hoffmann, R.; Fisel, C. R. *J. Am. Chem. Soc.*, in press.
(22) Curtis, M. D. "Abstracts of Papers", 11th Central Regional Meeting of the American Chemical Society, Columbus, Ohio, May 7-9, 1979; American Chemical Society: Washington, D.C., 1979.
(23) Adams, R. D.; Collins, D. E.; Cotton, F. A. *J. Am. Chem. Soc.* **1974**, *96*, 749-754.
(24) Goh, L.-Y.; D'Aniello, M. J., Jr.; Slater, S.; Muetterties, E. L.; Tavanaiepour, I.; Chang, M. I.; Fredrich, M. F.; Day, V. W. *Inorg. Chem.* **1979**, *18*, 192-197.
(25) Hackett, P.; O'Neill, P. S.; Manning, A. R. *J. Chem. Soc., Dalton Trans.* **1974**, 1625-1627.
(26) Unpublished calculations on the $[CpM(CO)_3]_2$ species have been performed in our group by D. L. Thorn.
(27) (a) Hoffmann, R. *J. Chem. Phys.* **1963**, *39*, 1397-1412. (b) Hoffmann, R.; Lipscomb, W. N. *Ibid.* **1962**, *36*, 2179-2189.
(28) Summerville, R. H.; Hoffmann, R. *J. Am. Chem. Soc.* **1976**, *98*, 7240-7254.

Evidence for the Incursion of Intermediates in the Hydrolysis of Tertiary, Secondary, and Primary Substrates

Michael Jesse Blandamer,[1a] Ross Elmore Robertson,* John Marshall William Scott,[1b] and Alice Vrielink[1c]

Contribution from the Chemistry Department, University of Calgary, Calgary, Alberta, Canada. *Received September 19, 1979*

Abstract: The temperature dependences related to a series of solvolytic displacement reactions of primary, secondary, and tertiary carbon centers are examined using a new equation. The equation is derived by integrating the van't Hoff isochore in a form related to the absolute rate theory on the assumption that the heat capacity of activation ($\Delta C_p^{\ddagger}$) is constant. Unexpectedly, the new equation is capable of correctly sensing changes in $\Delta C_p^{\ddagger}$ with temperature. The new equation is used to show that in some instances $\Delta C_p^{\ddagger}$ is partly abnormal and derives from the nonunitary nature of the displacements in a way outlined previously by Albery and Robinson. The significance of this new mechanistic tool is considered in relation to the displacement reaction of 2-bromopropane in heavy water and the reactions of adamantyl nitrate, *tert*-butyl chloride, *S*-propyl methanesulfonate, *m*-trifluoromethylbenzyl nitrate, and ethyl bromide with ordinary water.

Introduction

The temperature dependence of many ionogenic displacement reactions in water and mixed aqueous solvents is inadequately represented by the Arrhenius equation. The possible origins of such behavior have been the subject of a general review by Hulett[2a] and the displacement reactions have been specifically reviewed by Robertson[2] and Kohnstam[3] and form part of a more recent summary by Blandamer.[4] If the absolute rate theory formalism is adopted, then departures from the Arrhenius equation may be interpreted in terms of heat capacities of activation ($\Delta C_p^{\ddagger}$). For hydrolytic displacements of organic esters (RX)

$$RX + 2H_2O \rightarrow ROH + H_3O^+ + X^- \qquad (1)$$

the measured values of $\Delta C_p^{\ddagger}$ are invariably negative. Odd exceptions to this rule have their own particular explanation.[5]

The negative values of $\Delta C_p^{\ddagger}$ can be rationalized qualitatively in terms of various model processes. For example, the ionization reactions of amines and carboxylic acids are all characterized by negative ΔC_p° values. Likewise, the heat-capacity change for the hypothetical process

$$Ar(aq) \rightarrow Cl^-(aq) \qquad (2)$$

has been estimated to be negative.[6] These analogies draw attention to the solvation changes which characterize the activation of a neutral molecule (RX) to an ionic transition state which is postulated to show varying degrees of charge separation as the structures of R and X are changed.

The range of ΔC_p for many solvolytic substrates reacting in water is ca. -50 ± 30 cal mol^{-1} K^{-1} and this is consistent with the thermodynamic models mentioned above. Individual differences arising from structural alterations in the substrates (RX) have led to a variety of mechanistic speculations.[2b,3] Broadly speaking, such speculations have been related to the Ingold S_N1-S_N2 classification[7] together with the basic idea that S_N1 displacements demonstrate a greater sensitivity to solvation and are consequently characterized by more negative $\Delta C_p^{\ddagger}$ values. Many aspects of this picture are satisfactory; nevertheless, some nagging doubts remain.

For instance, a recent report[8] concerning the solvolysis of *t*-BuCl in *t*-BuOH gives a value of -627 cal mol^{-1} K^{-1} for $\Delta C_p^{\ddagger}$. The wholesale destruction of entropy which must be associated with such a large negative $\Delta C_p^{\ddagger}$ value is physically unreasonable. Similarly the hydrolyses of adamantyl nitrate[9] and *m*-trifluoromethylbenzyl nitrate[10] have respectively provided values of $\Delta C_p^{\ddagger}$ in the region of -150 cal mol^{-1} K^{-1} and these values are also outside the range of what might be anticipated reasonably on thermodynamic grounds.

One might argue that 1-adamantyl nitrate reacts only by a limiting (S_N1) mechanism and hence the large negative $\Delta C_p^{\ddagger}$ is that characteristic of a truly limiting displacement with the nitrate as a leaving group. However, the same mechanistic description for the substituted benzyl nitrate is not plausible. In the present paper we propose to seek alternative

0002-7863/80/1502-2585$01.00/0